

## Potential contributions of vertically migrating *Rhizosolenia* to nutrient cycling and new production in the open ocean

Tammi L. Richardson<sup>1</sup>, John J. Cullen, Dan E. Kelley and Marlon R. Lewis  
*Department of Oceanography, Dalhousie University, Halifax, NS B3H 4J1, Canada*

<sup>1</sup>*Present address: Department of Agricultural and Environmental Science, The Queen's University of Belfast, Newforge Lane, Belfast BT9 5PX, UK*

**Abstract.** We present a numerical model of nutrient uptake and photosynthesis during migrations of the marine diatom *Rhizosolenia* that was developed to estimate fluxes of carbon and nitrogen due to these migrations in the open ocean. The predicted specific rate of increase of *Rhizosolenia* was 0.11–0.15 day<sup>-1</sup>, whereas the total time for one migration cycle ranged between 3 and 5 days. Using published estimates of *Rhizosolenia* abundance, we estimate that new primary production due to *Rhizosolenia* migrations ranges between 0.018 and 0.033 mmol N m<sup>-2</sup> day<sup>-1</sup>. These values represent up to 17% of new production due to turbulent diffusive fluxes of nitrate into the euphotic zone and are of the same order of magnitude as new production due to nitrogen fixation in tropical oceans. Large-scale contributions of *Rhizosolenia* to oceanic new production are limited by their relatively low standing crop. Variations in the formulation of losses with depth greatly affected gross and net fluxes of carbon and nitrogen. Better characterization of losses of *Rhizosolenia* and improved estimates of its abundance will help determine more accurately the contributions of *Rhizosolenia* to global biogeochemical cycles.

### Introduction

Although open-ocean regions are often dominated by small plankton and food webs based on regenerated production (Eppley and Peterson, 1979), the occurrence and significance of large phytoplankton (>100 µm; after Goldman, 1988) in open-ocean regions are now well documented (Beers *et al.*, 1975; Alldredge and Silver, 1982; Goldman, 1988; Villareal, 1988; Karl *et al.*, 1992; Villareal *et al.*, 1993; Yoder *et al.*, 1994). Large phytoplankton typically found in these regions include the cyanobacterium *Trichodesmium* (e.g. Bowman and Lancaster, 1965; Villareal and Carpenter, 1990; Carpenter and Romans, 1991; Karl *et al.*, 1992) and diatoms of the genera *Ethmodiscus* and *Rhizosolenia* (e.g. Villareal, 1992; Villareal *et al.*, 1993). In general, open-ocean regions like the Central North Pacific Gyre are characterized by chronically low levels of nutrients in surface waters (Hayward, 1991; Karl *et al.*, 1992) which places large cells with small ratios of surface area to volume at a disadvantage in terms of nutrient uptake (Munk and Riley, 1952; Pasciak and Gavis, 1974; see also Chisholm, 1992). However, large phytoplankters found in these regions have developed mechanisms to cope with the scarcity of nutrients. *Trichodesmium*, for example, fixes atmospheric nitrogen, thus avoiding nitrogen limitation, and uses buoyancy reversals to migrate below the nutricline to acquire phosphorus (Carpenter and Romans, 1991; Karl *et al.*, 1992). Recent evidence supports the hypothesis (Villareal and Carpenter, 1989) that the mat-forming diatom *Rhizosolenia* and the single-celled diatom *Ethmodiscus* also use buoyancy reversals to undergo vertical migrations, allowing them to exploit sources of nutrients in deeper water (Villareal *et al.*,

1993; Villareal and Carpenter, 1994; Villareal and Lipschultz, 1995). For *Rhizosolenia*, this evidence includes  $\delta^{15}\text{N}$  signatures of surface-collected samples that are characteristic of cells that access deep-water sources of nutrients (Villareal *et al.*, 1993), and significantly higher internal nitrate concentrations in ascending cells than in sinking cells, consistent with the concept of nutrient replenishment by vertical movements between the surface and deep waters (Villareal *et al.*, 1993; Villareal and Lipschultz, 1995).

Uptake of nitrate by cells deep in the water column, followed by movement of cells from these nitrate-rich waters to nitrate-poor surface waters, results in the upward transport of nitrogen to the euphotic zone and thus is a form of new production (*sensu* Dugdale and Goering, 1967). The potential contribution of diatom migrations to new production and to the vertical flux of nutrients in the open ocean is not considered in current models of biogeochemical cycling (e.g. Fasham *et al.*, 1990). If cells are sufficiently abundant, the contributions may be important. Further, because nitrate transported to the surface by migrating diatoms may not be accompanied by stoichiometric equivalents of carbon, new production due to *Rhizosolenia* migrations can result in a disproportionately high net removal of carbon from oceanic surface waters (see Eppley and Peterson, 1979).

Central ocean gyres, where *Rhizosolenia* is most common, are significant contributors to the export of carbon from the euphotic zone, mostly due to their large geographical area (Martin *et al.*, 1987; Karl *et al.*, 1992). It is difficult to estimate the potential contributions of diatom migrations to biogeochemical cycling as data on the abundance of migrating diatoms in these regions, the amount of nutrient assimilation associated with each migration cycle, and the frequency of vertical cycling are rare or absent. Using data from field experiments (e.g. Villareal and Carpenter, 1989; Villareal *et al.*, 1996), along with data from laboratory experiments on nutrient uptake and photosynthesis in one species of *Rhizosolenia* (*Rhizosolenia formosa*) (Richardson *et al.*, 1996), we developed a numerical model of migrations of *Rhizosolenia* in a hypothetical open-ocean region. The model estimates fluxes of carbon and nitrogen due to *Rhizosolenia* migrations, the specific rate of increase of *Rhizosolenia* biomass, total migration cycle time, and the vertical distribution of a population of *Rhizosolenia* under steady-state conditions. Results were used to predict fluxes of carbon and nitrogen based on estimates of *Rhizosolenia* abundance from the field. We predict that contributions of *Rhizosolenia* migrations to open-ocean new production may represent up to 17% of new production that results from turbulent diffusion of nitrate into the euphotic zone.

### Description of the model

The model represents a community of *Rhizosolenia* mats in the upper water column of an oligotrophic open-ocean region (Figure 1). The general structure is based on a model by Kromkamp and Walsby (1990). *Rhizosolenia* biomass is represented as pools of particulate organic carbon (PC;  $\text{mmol m}^{-3}$ ) and particulate organic nitrogen (PN;  $\text{mmol m}^{-3}$ ) in 10 m intervals over the top 120 m of the water column. Nitrate is assumed to be zero in the upper 110 m, and then becomes

Potential contributions of *Rhizosolenia* to nutrient cycling

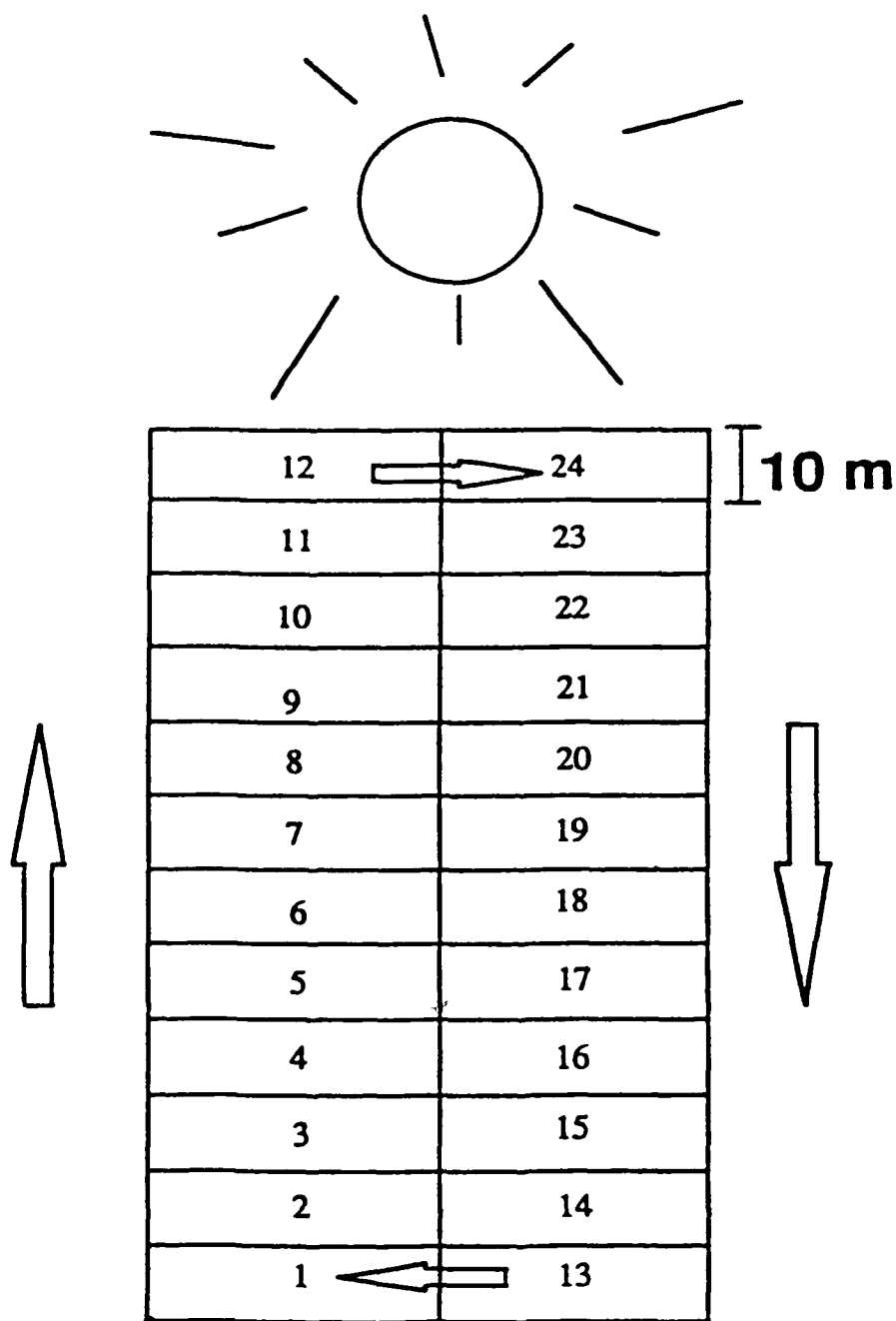


**Fig. 1.** Schematic of a box model of a *Rhizosolenia* migration cycle. Biomass ascends through boxes on the left side of the figure and sinks through boxes on the right side. Transfer of biomass from ascending to sinking paths (and vice versa) occurs only at the top and bottom boundaries. Irradiance is highest in the top layer and decreases exponentially with depth. Nitrate is available only in boxes 1 and 13.

available in unlimited supply only in the bottom layer of the modelled water column (110–120 m). This vertical structure is meant to reflect that found in oligotrophic regions of the world's oceans, where light and nutrients are spatially separated (see Hayward, 1991). Dissolved inorganic carbon is assumed to be in unlimited supply throughout the entire water column. Photosynthetically available radiation (PAR; after Morel, 1978) at the surface ( $I_0$ ;  $\mu\text{mol m}^{-2} \text{s}^{-1}$ ) varies with time of day according to:

$$I_0 = I_m \cdot \sin(\pi t/D) \quad \text{for } 0 < t < D \quad (1)$$

$$I_0 = 0 \quad \text{for } D < t < 24$$

(see Kirk, 1994) where  $I_m$  is the maximal irradiance at the sea surface at noon (assumed to be  $2000 \mu\text{mol m}^{-2} \text{s}^{-1}$ ),  $D$  is daylength (h; assumed to be 12 h) and  $t$  is time (h). The variation of irradiance with depth is described by:

$$I_z = I_0 \exp(-kz) \quad (2)$$

where  $z$  is depth (m),  $I_z$  is PAR ( $\mu\text{mol m}^{-2} \text{s}^{-1}$ ) at depth  $z$ , taken to be the irradiance at the depth of the middle of each layer, and  $k$  is the vertical attenuation coefficient for PAR ( $0.06 \text{ m}^{-1}$ , assumed to be constant with depth and with time). A complete list of symbols and parameters used in the model can be found in Table I.

**Table I.** Model variables and parameters. Multiple numbers in the value column refer to rates for nitrate-depleted and nitrate-replete biomass, respectively, and are used to define the range between which the actual value in the model varies [see equations (5), (6) and (7) in the text]

Symbol	Definition	Value	Units
$z$	depth		m
$I_z$	irradiance at depth $z$		$\mu\text{mol m}^{-2} \text{s}^{-1}$
$I_0$	surface irradiance	variable	$\mu\text{mol m}^{-2} \text{s}^{-1}$
$I_m$	maximum surface irradiance	2000	$\mu\text{mol m}^{-2} \text{s}^{-1}$
$D$	daylength	12	h
$t$	time		h
$\Delta z$	depth between layers	10	m
$k$	vertical attenuation coefficient	0.06	$\text{m}^{-1}$
$PC_n$	particulate carbon in box $n$		$\text{mmol m}^{-3}$
$PN_n$	particulate nitrogen in box $n$		$\text{mmol m}^{-3}$
$\Gamma_n$	absolute carbon uptake rate		$\text{mmol m}^{-3} \text{h}^{-1}$
$A$	ascent velocity	variable	$\text{m h}^{-1}$
$\Psi$	descent velocity	variable	$\text{m h}^{-1}$
$l_n$	specific loss rate in box $n$	variable	$\text{h}^{-1}$
$R_n$	respiration rate in box $n$	variable	$\text{h}^{-1}$
$P_n^N$	N-specific carbon uptake rate		$\text{mmol mmol}^{-1} \text{h}^{-1}$
$P_n^S$	maximum potential photosynthesis rate	0.1–0.2	$\text{mmol mmol}^{-1} \text{h}^{-1}$
$\alpha^N$	initial slope of the $P-I$ curve	0.0015–0.0019	$\text{mmol mmol}^{-1} \text{h}^{-1} (\mu\text{mol m}^{-2} \text{s}^{-1})^{-1}$
$\beta^N$	photoinhibition parameter	$1.5 \times 10^{-5}$ – $5.2 \times 10^{-5}$	$\text{mmol mmol}^{-1} \text{h}^{-1} (\mu\text{mol m}^{-2} \text{s}^{-1})^{-1}$
$\Omega_n$	absolute nitrate uptake rate		$\text{mmol m}^{-3} \text{h}^{-1}$
$V$	N-specific nitrate uptake rate	0.02	$\text{h}^{-1}$

Changes in PC and PN in each layer are the net result of several processes: (i) photosynthesis or nitrate uptake; (ii) increases or decreases in PC or PN due to movements of biomass into or out of the layer; (iii) losses from the layer due to grazing, cell lysis, irreversible sinking of biomass and, for the case of PC only, cell respiration.

### Photosynthesis

Absolute carbon uptake,  $\Gamma_n$  ( $\text{mmol m}^{-3} \text{ h}^{-1}$ ), is defined as:

$$\Gamma_n = P^N \cdot PN_n \quad (3)$$

where  $PN_n$  is the concentration of PN ( $\text{mmol m}^{-3}$ ) in box  $n$  and  $P^N$  is the nitrogen-specific carbon uptake rate ( $\text{mmol mmol}^{-1} \text{ h}^{-1}$ ) formulated according to the equation of Platt *et al.* (1980):

$$P^N = P_S^N (1 - e^{(-\alpha^N I_z / P_S^N)}) (e^{(-\beta^N I_z / P_S^N)}) \quad (4)$$

except that  $P^N$  is the rate of photosynthesis normalized to PN rather than to chlorophyll,  $P_S^N$  is the maximum rate of photosynthesis in the absence of photo-inhibition ( $\text{mmol mmol}^{-1} \text{ h}^{-1}$ ),  $I_z$  is irradiance ( $\mu\text{mol m}^{-2} \text{ s}^{-1}$ ) at depth  $z$ ,  $\alpha^N$  is the initial slope of the photosynthesis-irradiance ( $P-I$ ) curve [ $\text{mmol mmol}^{-1} \text{ h}^{-1} (\mu\text{mol m}^{-2} \text{ s}^{-1})^{-1}$ ] and  $\beta^N$  is a parameter that characterizes photoinhibition [ $\text{mmol mmol}^{-1} \text{ h}^{-1} (\mu\text{mol m}^{-2} \text{ s}^{-1})^{-1}$ ].

Values used for the parameters  $P_S^N$ ,  $\alpha^N$ , and  $\beta^N$  were determined experimentally by Richardson *et al.* (1996) (see Table I). These values were determined at 20°C; thus, the values for  $P_S^N$  in the surface (0–10 m) layer were multiplied by a  $Q_{10}$  of 2.6 (the expected increase in maximal photosynthetic rate for a 10°C increase in temperature; see Li and Morris, 1982) to account for expected increases in  $P_S^N$  due to higher surface temperatures in the Central North Pacific Gyre (e.g. Hayward, 1991). Values determined for the photosynthetic parameters during laboratory experiments also varied depending on whether the biomass was nitrate replete (and thus with a low C:N ratio) or nitrate depleted (higher C:N) (see Richardson *et al.*, 1996). Thus, in the model,  $P_S^N$  varied as a function of the PC:PN ratio according to:

$$P_S^N = 0.29 + (-0.012 \cdot PC_n / PN_n) \quad (5)$$

while  $\alpha^N$  varied according to:

$$\alpha^N = 0.002 + (-4 \times 10^{-5} \cdot PC_n / PN_n) \quad (6)$$

and  $\beta^N$  varied according to:

$$\beta^N = (8.2 \times 10^{-5}) + (-4.4 \times 10^{-6} \cdot PC_n / PN_n) \quad (7)$$

Equations (5), (6) and (7) are the equations that describe a linear increase or decrease in the parameter of interest between the range of values shown in Table I. They are constrained by experimental measurements of the *P-I* parameters of nitrate-replete and nitrate-depleted *R.formosa* taken from Richardson *et al.* (1996).

#### *Nitrate uptake*

Absolute nitrate uptake rate ( $\Omega_n$ ) was defined as:

$$\Omega_n = V \cdot PN_n \quad (8)$$

where  $V$  is the N-specific uptake rate ( $\text{h}^{-1}$ ). Nitrate uptake rates used for the model were determined experimentally for *R.formosa* (Richardson *et al.*, 1996);  $V$  was set to a constant value of  $0.02 \text{ h}^{-1}$  as Richardson *et al.* (1996) showed that the N-specific nitrate uptake rate of this diatom did not vary significantly with nutritional state or with incubation of cells in the light or in the dark. We also assume that the specific nitrate uptake rate does not vary with temperature. This value represents the average N-specific uptake rate determined during a 12 h incubation and is not a maximal or a steady-state uptake rate. A specific uptake rate of  $0.02 \text{ h}^{-1}$  allows luxury consumption of nitrate, i.e. cells can take up nitrate in excess of their immediate metabolic requirements (see Richardson *et al.*, 1996).

#### *Movements of biomass*

The light and nutrient history of *Rhizosolenia* greatly influences whether cells are positively or negatively buoyant and the velocity with which cells ascend or sink through the water column (see Moore and Villareal, 1996a; Richardson *et al.*, 1996; Villareal *et al.*, 1996). In the model, we used the PC:PN ratio, which reflects light and nutrient history, to determine when biomass would switch between positive and negative buoyancy. That is, the PC:PN ratio determined when biomass would sink from the surface (0–10 m) layer and when biomass would ascend from the deepest (110–120 m) layer of the model. The base model was formulated such that biomass sank from the surface only when the molar ratio of PC:PN was  $>11.9$ ; biomass ascended from the deepest layer only when the molar ratio of PC:PN was  $<8.3$ . Biomass accumulated in the surface or deepest layers until ratios reached these critical values. Parameterization of the critical values for the base model was based on C:N ratios of *Rhizosolenia* mats collected in the field by Villareal *et al.* (1996).

The ratio of PC:PN was also used to determine the velocity with which biomass ascended or sank between layers in the model. Ascent velocity ( $A$ ;  $\text{m h}^{-1}$ ) was determined according to:

$$A = A'[13 - (PC_n/PN_n)] \quad (9)$$

where  $PC_n$  is the concentration of PC ( $\text{mmol m}^{-3}$ ) in box  $n$  and  $A'$  is a constant value of  $1 \text{ m h}^{-1}$ . According to equation (9), ascent velocity goes to zero when the

molar PC:PN ratio increases to 13, as would happen during nitrate starvation. During simulations, ascent velocities were never negative because ascending biomass did not exceed molar C:N ratios of 13. Descent velocity ( $\Psi$ ; m h<sup>-1</sup>) was similarly defined as a function of molar PC:PN ratio:

$$\Psi = \Psi'[(PC_n/PN_n) - 8.3] \quad (10)$$

where  $\Psi'$  is a constant value of 1 m h<sup>-1</sup>. As above, descent velocities were never negative as the molar PC:PN ratio of the descending biomass did not fall below 8.3 during the descent. Equations (9) and (10) were formulated such that ascent and descent velocities were within the range of those measured previously in the field for mats of *Rhizosolenia* (Villareal and Carpenter, 1989; Villareal *et al.*, 1996). We varied the velocities as a function of PC:PN ratio because laboratory observations of *R. formosa* showed that cells with higher C:N ratios had higher estimated sinking velocities (Richardson *et al.*, 1996; see their Figure 3). For positively buoyant biomass, we have made the assumption that *Rhizosolenia* will slow their ascent velocity as their PC:PN ratio increases nearer to the surface, due to increased photosynthetic rates, decreased availability of nutrients, and thus increased production of carbohydrate (see Richardson and Cullen, 1995; Richardson *et al.*, 1996). Because velocities were functions of the PC:PN ratio, they changed as the ratio changed on a diel basis and due to migration to more highly illuminated layers, or to the nitrate-rich deep layer of the model. The movements of PC and PN were always coupled; changes in the ratio of PC:PN in any layer, therefore, were due only to varying rates of photosynthesis and nitrate uptake. Finally, we assume that the PC:PN ratio reflects the primary determinants of both the direction and velocity of movement. We represent ascent and descent velocities as distinct mathematical functions to account for factors other than changes in chemical composition (e.g. cellular ion content; see Smayda, 1970) that are physiologically related to the PC:PN ratio and which may influence cell buoyancy.

### Losses

We have combined losses due to grazing, cell lysis and irreversible sinking of biomass into one loss term, expressed as a specific loss rate:  $l_n$  (h<sup>-1</sup>). In the base model, the specific loss rate was assumed to be constant with depth. For each simulation, the value of  $l_n$  was adjusted iteratively so that losses balanced increases in surface PC and PN for at least five successive migration cycles; when losses balanced increases in surface PC and PN the model was deemed to be in steady state. The model thus calculates the specific rate of increase (which equals the specific loss rate, h<sup>-1</sup>, converted to day<sup>-1</sup> for comparison purposes). Losses due to cell respiration, applied using a specific respiration rate,  $R_n$  (h<sup>-1</sup>), were to the PC pool only. These were accounted for by first running the model with  $R_n$  set to zero, then re-running the model with  $R_n$  equal to 10% of the specific rate of increase determined by the previous model run. The choice of 10% was based on Geider (1992) and Cullen *et al.* (1993).

*General equations*

Laboratory (Richardson *et al.*, 1996) and field (Villareal *et al.*, 1996) studies have shown that positively buoyant *Rhizosolenia* (ascending cells or mats) differ in physiology and chemical composition from those that are negatively buoyant. Thus, we modelled ascending biomass separately from sinking biomass (as is shown in Figure 1) so that we could apply values of photosynthetic parameters that were appropriate to the physiological state of the biomass (i.e. nitrate replete versus nitrate depleted). The total biomass at each depth in the model, therefore, is the sum of the ascending and sinking biomass. For ascending biomass (boxes on the left-hand side of Figure 1, excluding boundary boxes 1 and 12), the general equations describing changes in PC and PN are:

$$\frac{dPC_n}{dt} = \{\Gamma_n + [(A_{n-1}/\Delta z) \cdot PC_{n-1}]\} - \{[(A_n/\Delta z) \cdot PC_n] + [l_n \cdot PC_n] + [R_n \cdot PC_n]\} \quad (11)$$

and

$$\frac{dPN_n}{dt} = \{\Omega_n + [(A_{n-1}/\Delta z) \cdot PN_{n-1}]\} - \{[(A_n/\Delta z) \cdot PN_n] + [l_n \cdot PN_n]\} \quad (12)$$

where  $PC_n$  and  $PN_n$  are the concentrations of PC and PN ( $\text{mmol m}^{-3}$ ) in box  $n$  (as above),  $PC_{n-1}$  and  $PN_{n-1}$  are the concentrations of PC and PN in box  $n-1$  (which is below box  $n$ ),  $A_n$  is the ascent velocity of material leaving box  $n$  ( $\text{m h}^{-1}$ ) (as above),  $A_{n-1}$  is the ascent velocity of material moving up from box  $n-1$  ( $\text{m h}^{-1}$ ) and  $\Delta z$  is the depth interval between boxes (10 m).

For sinking biomass (boxes on the right-hand side of Figure 1, excluding boundary boxes 13 and 24), changes in PC and PN are described by:

$$\frac{dPC_n}{dt} = \{\Gamma_n + [(\Psi_{n+1}/\Delta z) \cdot PC_{n+1}]\} - \{[(\Psi_n/\Delta z) \cdot PC_n] + [l_n \cdot PC_n] + [R_n \cdot PC_n]\} \quad (13)$$

and

$$\frac{dPN_n}{dt} = \{\Omega_n + [(\Psi_{n+1}/\Delta z) \cdot PN_{n+1}]\} - \{[(\Psi_n/\Delta z) \cdot PN_n] + [l_n \cdot PN_n]\} \quad (14)$$

where  $PC_{n+1}$  and  $PN_{n+1}$  are the concentrations of PC and PN ( $\text{mmol m}^{-3}$ ) in box  $n+1$ , the next box above box  $n$ ,  $\Psi_n$  is the descent velocity of material from box  $n$  ( $\text{m h}^{-1}$ ) and  $\Psi_{n+1}$  is the descent velocity of material from box  $n+1$  into box  $n$ .

*Boundary conditions, initial conditions and other assumptions*

We assume that there is no exchange of material across the air/sea interface, no horizontal advection, and that there is no exchange between ascending and sinking biomass except at the top (0–10 m) and bottom (110–120 m). Changes in PC and PN in the top boundary boxes (boxes 12 and 24 in Figure 1) and in the bottom boundary boxes (1 and 13 in Figure 1) are described by equations presented in Table II.

We consider only the contributions of *Rhizosolenia* to carbon and nitrogen fluxes, and assume that diffusive and advective fluxes of nitrate are negligible, and that advective processes do not significantly influence the movement of diatoms. The growth of *Rhizosolenia* is assumed to be dependent entirely on nitrate; we do not consider the possibility of ammonia-based growth. Finally, we assume that these *Rhizosolenia* contain no nitrogen-fixing endosymbionts (see Alldredge and Silver, 1982; Martinez *et al.*, 1983; cf. Villareal, 1987; Villareal and Carpenter, 1989).

The model was started with biomass distributed evenly from top to bottom in a molar PC:PN ratio of 8.3. Variations in the initial distribution of the biomass or in the initial PC:PN ratio did not alter the final results of the model. The initial abundance of PN (0.022 mmol m<sup>-2</sup>) was taken from published data on *Rhizosolenia* mats in the Central North Pacific Gyre (Villareal and Carpenter, 1989), calculated

**Table II.** Equations describing changes in particulate carbon (PC; mmol m<sup>-3</sup>) and particulate nitrogen (PN; mmol m<sup>-3</sup>) in the boundary boxes of the *Rhizosolenia* model. Numbers in subscript refer to the boxes as shown in Figure 1. As in the text, *t* is time (h),  $\Gamma$  is the absolute carbon uptake (mmol m<sup>-3</sup> h<sup>-1</sup>), *A* is the ascent velocity (m h<sup>-1</sup>),  $\Psi$  is the descent velocity (m h<sup>-1</sup>),  $\Omega$  is the absolute nitrate uptake rate (mmol m<sup>-3</sup> h<sup>-1</sup>),  $\Delta z$  is the depth interval between boxes (10 m), *R* is the specific respiration rate (h<sup>-1</sup>) and *l* is the specific loss rate (h<sup>-1</sup>). The equations describe increases in biomass due to photosynthesis or nitrate uptake, and increases or decreases due to transfer of biomass to descending or ascending streams of phytoplankton as shown in Figure 1. The expressions  $\frac{1}{2} \cdot PC_n$  and  $\frac{1}{2} \cdot PN_n$  (where *n* is the number of the appropriate box) represent the amount of biomass transferred between boxes in the same layer, i.e. one half of the biomass was transferred every hour. The specific transfer rate of  $\frac{1}{2}$  was chosen so that PC:PN ratios did not exceed the range of possible values established experimentally. Specific transfer rates greater than  $\frac{1}{2}$  did not noticeably affect the outcome of the model

Box	Equation
12	$\frac{dPC_{12}}{dt} = \{\Gamma_{12} + [(A_{11}/\Delta z) \cdot PC_{11}]\} - \{[\frac{1}{2} \cdot PC_{12}] + [l_{12} \cdot PC_{12}] + [R_{12} \cdot PC_{12}]\}$ $\frac{dPN_{12}}{dt} = \{\Omega_{12} + [(A_{11}/\Delta z) \cdot PN_{11}]\} - \{[\frac{1}{2} \cdot PN_{12}] + [l_{12} \cdot PN_{12}]\}$
24	$\frac{dPC_{24}}{dt} = \{\Gamma_{24} + [\frac{1}{2} \cdot PC_{12}]\} - \{[(\Psi_{24}/\Delta z) \cdot PC_{24}] + [l_{24} \cdot PC_{24}] + [R_{24} \cdot PC_{24}]\}$ $\frac{dPN_{24}}{dt} = \{\Omega_{24} + [\frac{1}{2} \cdot PN_{12}]\} - \{[(\Psi_{24}/\Delta z) \cdot PN_{24}] + [l_{24} \cdot PN_{24}]\}$
1	$\frac{dPC_1}{dt} = \{\Gamma_1 + [\frac{1}{2} \cdot PC_{13}]\} - \{[(A_1/\Delta z) \cdot PC_1] + [l_1 \cdot PC_1] + [R_1 \cdot PC_1]\}$ $\frac{dPN_1}{dt} = \{\Omega_1 + [\frac{1}{2} \cdot PN_{13}]\} - \{[(A_1/\Delta z) \cdot PN_1] + [l_1 \cdot PN_1]\}$
13	$\frac{dPC_{13}}{dt} = \{\Gamma_{13} + [(\Psi_{14}/\Delta z) \cdot PC_{14}]\} - \{[\frac{1}{2} \cdot PC_{13}] + [l_{13} \cdot PC_{13}] + [R_{13} \cdot PC_{13}]\}$ $\frac{dPN_{13}}{dt} = \{\Omega_{13} + [(\Psi_{14}/\Delta z) \cdot PN_{14}]\} - \{[\frac{1}{2} \cdot PN_{13}] + [l_{13} \cdot PN_{13}]\}$

from average values of  $0.3 \text{ mats m}^{-3}$  and a nitrogen content of  $2.5 \times 10^{-3} \text{ mmol mat}^{-1}$  (Villareal and Carpenter, 1989) integrated to a depth of 30 m. The initial molar PC content was calculated by multiplying the initial PN by 8.3.

#### *Variations in the base model*

To test the sensitivity of the model to changes in various parameters, we altered the base model by changing either the function that determines ascent or descent velocities, the critical values of PC:PN at which biomass sinks from the top or floats up from the bottom layer, or the vertical distribution of losses.

The effects of variations in ascent and descent velocities were determined by setting ascent and descent velocities to constant values of 3, 6 and  $8 \text{ m h}^{-1}$  instead of making them functions of the PC:PN ratio as in the base model, but the critical PC:PN ratios for sinking and floating were still applied. The range of ascent and descent velocities was based on data for mats of *Rhizosolenia* in the Central North Pacific Gyre (Villareal and Carpenter, 1989; Villareal *et al.*, 1996). The velocity of  $8 \text{ m h}^{-1}$  is among the highest of ascent rates determined for *Rhizosolenia* in the field (see Moore and Villareal, 1996b) and is probably extreme.

To test the sensitivity of the model to the choice of C:N criteria for sinking or floating, the critical C:N was varied as shown in Table III. The choice of variations of the critical values was based partly on the range of C:N ratios of sinking and floating mats of *Rhizosolenia* in the Central North Pacific Gyre (Villareal *et al.*, 1996) and partly on the minimum and maximum values of molar C:N (7 and 15, respectively) obtained for N-replete and N-depleted cultures of *R. formosa* grown in the laboratory (Richardson *et al.*, 1996).

The base model had losses occurring equally from all depths. To test the sensitivity of the model to variations in specific loss rate with depth, the value of the loss term was adjusted so that losses occurred (i) only from the top layer of the model (i.e. the specific loss rate of all other boxes was set to zero), (ii) only from the bottom layer of the model or (iii) from the top and bottom layers only, but not from the middle layers. As with the base model, the specific loss rate was adjusted to balance gains in surface PC and PN.

#### **Calculations**

Equations were solved by Euler integration with a time step of 0.25 h using Stella for Macintosh, Version 2.2.1. Each model was run for 900 h of migration cycle

**Table III.** Variations of the critical molar particulate carbon:particulate nitrogen (PC:PN) ratios for sinking and floating

PC:PN cue to sink	PC:PN cue to float
PC:PN > 11.9 (Base model)	PC:PN < 8.3 (Base model)
PC:PN > 10.7	PC:PN < 7.1
PC:PN > 15.4	PC:PN < 8.3

time (~9 full cycles). Output from the model made possible the calculation of (i) fluxes of PC and PN, (ii) specific rates of increase, (iii) migration cycle times and (iv) vertical distributions of PC and PN.

We calculated upward and downward fluxes of PC and PN across the 110 m interface as the product of the ascent or descent velocity and the concentration of biomass in each relevant box at time intervals of 0.5 h. Average flux was calculated for an entire migration cycle and was expressed as  $\text{mmol C}$  or  $\text{mmol N m}^{-2} \text{ day}^{-1}$ . Then, since there were small variations in the fluxes, an overall average was calculated for the last three migration cycles of the model run. Two types of fluxes were calculated, gross and net; net flux was the difference between gross upward and downward fluxes.

Particulate C and PN were initially uniform with depth. Once in steady state, the time required for biomass to reach critical PC:PN ratios for sinking and floating caused accumulations of biomass in the top and bottom layers. We determined total migration cycle times by calculating the time difference between peaks of surface PC and PN; these were confirmed by calculating the time difference between peaks of upward and downward fluxes of biomass.

We calculated the average vertical distribution of biomass in the model by recognizing that, at steady state, average biomass found at each depth interval, as a proportion of integral biomass, is equivalent to the residence time in that interval. We integrated biomass at each depth interval with respect to time over a migration cycle, and divided it by the integral biomass times the total cycle time. These values (proportions) were expressed as distributions of PC and PN with depth.

## Results

### Base model predictions

Using the initial biomass of  $0.18 \text{ mmol C m}^{-2}$  and  $0.022 \text{ mmol N m}^{-2}$ , the base model predicted a net downward flux of PC of  $0.012 \text{ mmol m}^{-2} \text{ day}^{-1}$  and a net upward flux of PN of  $0.003 \text{ mmol m}^{-2} \text{ day}^{-1}$  (Table IV). The specific rate of

**Table IV.** Predicted upward, downward and net fluxes of particulate carbon (PC) and particulate nitrogen (PN), specific rates of increase, and total migration cycle times with variations in ascent and descent velocities used in the model

Flux ( $\text{mmol m}^{-2} \text{ day}^{-1}$ )	Base model	3 m $\text{h}^{-1}$	6 m $\text{h}^{-1}$	8 m $\text{h}^{-1}$
Upward PC	0.080	0.067	0.124	0.121
Downward PC	0.092	0.077	0.143	0.143
Net flux PC (down)	0.012	0.010	0.019	0.022
Upward PN	0.010	0.009	0.016	0.016
Downward PN	0.007	0.006	0.012	0.012
Net flux PN (up)	0.003	0.003	0.004	0.004
Specific rate of increase ( $\text{day}^{-1}$ )	0.12	0.11	0.14	0.15
Total migration cycle time (days)	4	5	3	3

increase predicted by the model was  $0.12 \text{ day}^{-1}$ , while the total migration cycle time was predicted to be 4 days. The predicted vertical distribution of PC was ~22% in the surface 10 m, 26% in the bottom 10 m (Table V), with the remainder of the biomass distributed approximately evenly through the water column. Particulate N had a similar predicted distribution, with 21% of the PN being found in the surface layer and 28% in the bottom layer (Table V). As with PC, the remainder of the biomass was distributed approximately evenly through the remainder of the water column. An uncoupling of the distribution of PN from PC was observed, i.e. the percentage of PN found in the deepest layer was higher than the percentage of PC; the opposite was true for the surface layer (Table V). Thus, molar C:N ratios of biomass decreased with depth to 7.1 from 15.

#### *Variations in ascent and descent velocities*

Variations in ascent and descent velocities affected the fluxes of PC and PN (Figure 2), the specific rate of increase, the total migration cycle time (Table IV) and the predicted vertical distribution of PC and PN (Table V). Net flux of PC was in the downward direction and increased with increasing ascent and descent velocity (Figure 2). Net flux of PN was in the upward direction; net flux increased with increasing ascent and descent velocities until rates of  $6 \text{ m h}^{-1}$ , after which there was no increase in the net upward flux of N. Total migration cycle time decreased with increasing ascent and descent velocities until  $6 \text{ m h}^{-1}$ , beyond which changes were small. Specific rates of increase predicted by the model increased slightly with increased ascent and descent velocities. As ascent and descent velocities increased, the vertical distribution of biomass was affected such that higher percentages of biomass were found at the surface and in the deepest layer (Table V). All ascent and descent velocity variations showed an uncoupling between the percentages of PC and PN found at the surface and in the deep boxes, as described for the base model, above.

#### *Variations in critical C:N for sinking and floating*

Variations in the critical C:N ratio at which biomass sank or floated affected the predicted vertical distribution of biomass (Table V). The lower or higher the critical C:N, the longer the amount of time required in the surface or deep box,

**Table V.** Predicted vertical distributions represented as a percent of total *Rhizosolenia*-derived particulate carbon (PC) and particulate nitrogen (PN) for the base model and variations thereof. For all cases, biomass not found in the top or bottom layer was distributed evenly between layers at mid-depths

Model	Base model	A, $\Psi = 3 \text{ m h}^{-1}$	A, $\Psi = 6 \text{ m h}^{-1}$	A, $\Psi = 8 \text{ m h}^{-1}$	Critical PC:PN 10.7, 7.1	Critical PC:PN 15.4, 8.3	Top loss only	Bottom loss only	Top & bottom loss
PC Top 10 m	22	23	25	32	15	39	21	20	20
PC Bottom 10 m	26	23	31	33	38	29	25	25	25
PN Top 10 m	21	21	24	32	15	36	20	20	20
PN Bottom 10 m	28	24	32	34	41	30	26	27	27

Potential contributions of *Rhizosolenia* to nutrient cycling

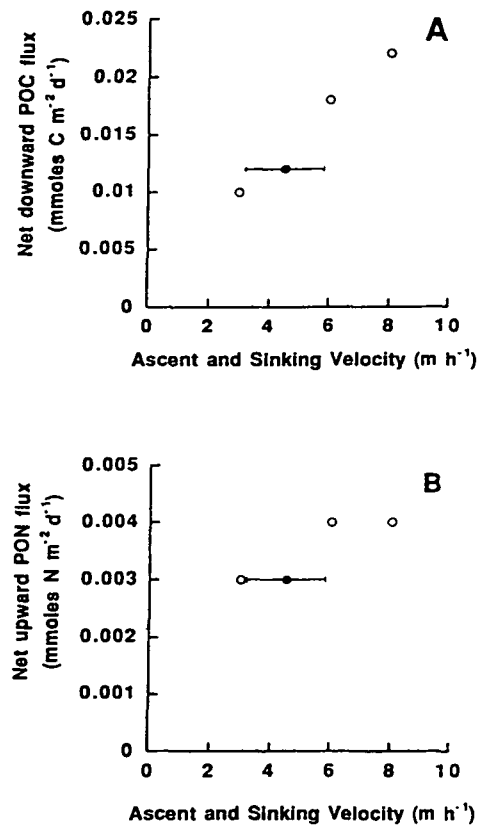


Fig. 2. (A) Net downward flux of particulate carbon and (B) net upward flux of particulate nitrogen for the base model (solid symbols) and for models where ascent and descent velocity are set at constant values of 3, 6 and 8 m h<sup>-1</sup>. Horizontal bars on the solid symbols show the range of variation of ascent and descent velocities used for flux calculations in the base model.

respectively, to reach the critical C:N, the greater the percentage of total migration cycle time spent in the box, and therefore the greater the predicted percentage of biomass found in the box. A greater difference between critical C:N ratios resulted in more time being spent in the top and bottom boxes (and less time at mid-depths), and therefore a greater percentage of total PC and PN in the top and bottom boxes (see Table V).

Variations in the C:N ratio at which biomass sank or floated affected, to some extent, the magnitude of the predicted flux of PC, although there was no detectable difference in the flux of PN (Table VI). The total time for one migration cycle increased slightly compared to the base model when the critical molar C:N ratios were changed to 10.7 (for sinking) and 7.1 (for floating) and to 15.4 (for sinking) and 8.3 (for floating) from values of 11.9 and 8.3 for sinking and floating, respectively. Increases in the specific rate of increase were detected only when the critical C:N ratio for sinking was increased to 15.4.

**Table VI.** Predicted upward, downward and net fluxes of particulate carbon (PC) and particulate nitrogen (PN), specific rates of increase, and migration cycle times for variations in the critical molar PC:PN ratios for sinking and floating

Flux (mmol m <sup>-2</sup> day <sup>-1</sup> )	PC:PN sink = 11.9 PC:PN float = 8.3 Base model	PC:PN sink = 10.7 PC:PN float = 7.1	PC:PN sink = 15.4 PC:PN float = 8.3
Upward PC	0.080	0.065	0.064
Downward PC	0.092	0.080	0.079
Net flux PC (down)	0.012	0.015	0.015
Upward PN	0.010	0.010	0.008
Downward PN	0.007	0.007	0.005
Net flux PN (up)	0.003	0.003	0.003
Specific rate of increase (day <sup>-1</sup> )	0.12	0.12	0.14
Total migration cycle time (days)	4	4.3	5

*Variation in the amplitude of the loss term with depth*

Variation in the amplitude of the loss term with depth greatly affected the magnitude of the net fluxes of PC and PN (Table VII). For example, losses concentrated in the top layer resulted in a noticeable reduction of net downward flux of PC compared to the base model, but a slightly enhanced net upward flux of PN (Table VII). Concentration of losses in the bottom layer of the model resulted in enhanced net downward flux of PC compared to the base model, but reduced the net upward flux of PN to zero (Table VII). As with all other models, the percentage of PC predicted for the surface layer was higher than the percentage of PN, but higher PN than PC was predicted for the deepest box.

**Table VII.** Predicted upward, downward and net fluxes of particulate carbon (PC) and particulate nitrogen (PN), specific rates of increase, and total migration cycle times with variations in the vertical distribution of losses

Flux (mmol m <sup>-2</sup> day <sup>-1</sup> )	Losses even with depth (Base model)	Top losses only	Bottom losses only	Top and bottom loss
Upward PC	0.080	0.088	0.094	0.094
Downward PC	0.092	0.089	0.152	0.123
Net flux PC (down)	0.012	0.001	0.058	0.029
Upward PN	0.010	0.011	0.012	0.012
Downward PN	0.007	0.007	0.012	0.010
Net flux PN (up)	0.003	0.004	0	0.002
Specific rate of increase (day <sup>-1</sup> )	0.12	0.12	0.12	0.12
Total migration cycle time (days)	4	4	4	4

## Discussion

Our model predicts that the time for one migration cycle of *Rhizosolenia* is between 3 and 5 days. These values agree well with those of Villareal *et al.* (1996), who calculated a range of 3.6–5.4 days for migration cycle times based on measurements of photosynthetic rates, ascent and descent velocities, estimates of nitrate uptake rates, and an implicit assumption of one migration cycle per generation time. In general, the total time for one migration cycle predicted by the model was shorter when ascent and descent velocities were increased, but only for increases up to values of 6 m h<sup>-1</sup>. Above this velocity, the time required for *Rhizosolenia* to reach critical C:N ratios in the top and bottom layers set limitations on how fast the migration cycle could be completed. The time to reach critical PC:PN ratios also affected the net upward flux of PN. Increasing the ascent velocity past 6 m h<sup>-1</sup> did not result in an increased flux of PN because the biomass was still ‘waiting’ in the bottom layer to reach the critical C:N for floating.

We predict specific rates of increase of *Rhizosolenia* to be between 0.11 and 0.15 day<sup>-1</sup>. These values agree well with growth rates determined for *R. formosa* in the laboratory by Richardson *et al.* (1996), but are lower than those predicted by Moore and Villareal (1996a) (~0.24 day<sup>-1</sup>) for growth of *R. formosa* at similar irradiance. The reason for the discrepancy is not clear. We expect that higher growth rates will increase the contributions of *Rhizosolenia* to nutrient cycling, but the exact contributions cannot be calculated using our model in its present form.

Rates of nitrate uptake and photosynthesis used for model parameters were based on laboratory experiments with monospecific cultures of *R. formosa* grown at a relatively low irradiance and low temperature (50 μmol m<sup>-2</sup> s<sup>-1</sup> and 20°C; Richardson *et al.*, 1996), conditions that differ from those in the field. *Rhizosolenia* mats found in the open ocean are composed of several species, some of which are larger than *R. formosa* and which may vary with respect to growth rate and photosynthetic physiology (see Moore and Villareal, 1996a). We acknowledge the differences between relatively small, monospecific cultures and multi-species mats of *Rhizosolenia*, but justify the use of laboratory-determined rates because, for the case of the nitrate uptake rates, no other data were available. As well, we applied a  $Q_{10}$  to the maximum photosynthetic rates of biomass in the surface layer of the model to bring these values within the range of rates determined for *Rhizosolenia* collected from higher temperature surface water in the field. In comparable units, our surface  $P_{\max}$  value for N-replete cells (including the  $Q_{10}$  adjustment) was 6.8 g C g<sup>-1</sup> Chl day<sup>-1</sup>, which compares well to Alldredge and Silver’s (1982) estimate of 5.8 g C g<sup>-1</sup> Chl day<sup>-1</sup> for cells collected from the North Pacific Ocean and to a measurement of 5.7 g C g<sup>-1</sup> Chl day<sup>-1</sup> for cells collected in the Equatorial Pacific Ocean (Yoder *et al.*, 1994).

We assumed that the net growth of *Rhizosolenia* was entirely dependent on nitrate and that the use of ammonia was negligible. The nitrogen preferences of *Rhizosolenia* have not been investigated; however, the δ<sup>15</sup>N signature of material collected in the field (Villareal *et al.*, 1993), as well as high intracellular concentrations of nitrate (Villareal and Lipschultz, 1995), suggest that deep-water nitrate is the main source of nitrogen used for growth (see also Villareal *et al.*, 1996).

The vertical distribution of *Rhizosolenia* in steady state was affected by variations in ascent and descent velocities, and by variations in the critical C:N ratios for sinking and floating. Generally, as ascent and descent velocities increased, smaller percentages of biomass were found at mid-depths, consistent with faster transit times between top and bottom layers. The critical C:N ratios influenced how much time in the top and bottom boxes was required by *Rhizosolenia* to reach the critical ratios, and therefore the expected vertical distribution of biomass. Vertical distributions predicted by the model are only partly supported by observations in the field. Accumulations of *Rhizosolenia* at the surface have been reported (Alldredge and Silver, 1982; Martinez *et al.*, 1983; Villareal and Carpenter, 1989; Villareal *et al.*, 1993, 1996), especially during periods of low winds over several days (Villareal *et al.*, 1996). This is consistent with the predicted accumulation of *Rhizosolenia* in the top 10 m of the model. To date, however, no accumulations of biomass have been found near the top of the nutricline; accumulations predicted by the model are at least partly caused by the closed bottom boundary.

Perhaps the greatest potential source of error in this model is that we have assumed that the effects of physical forcing, such as advection, upwelling or turbulence, on the movements of biomass from one depth horizon to another are negligible. This assumption is valid only when there is low wind-induced turbulence and relatively shallow surface mixed layers, conditions where the physiologically induced buoyancy changes override movements of cells by physical forcing. Surface mixed layers are shallow (10–20 m) in the North Pacific Central Gyre during the summer months (see Hayward, 1994) and it is under these conditions that the accumulations of *Rhizosolenia* biomass (discussed above) are found. Thus, this assumption is acceptably valid. The effects of physical processes on the vertical distribution of biomass would be to distribute the biomass more evenly through the water column. It is difficult to predict how the effects of physical forcing would affect the predicted fluxes of C and N, and it is clearly an avenue that requires further investigation.

Fluxes of PC and PN due to migrations of *Rhizosolenia* were more greatly affected by variations in the application of losses with depth than by variations in any other component of the model. In general, the distribution of losses with depth affected the magnitude of both gross and net fluxes due to differential effects on gains and losses of biomass. For example, concentration of losses in the surface layer reduced the net downward flux of PC (compared to the base model where losses were uniform with depth) because the losses were applied directly to the layer where the gains of PC were the highest.

It is difficult to know how to apply losses properly in the model, as very little information exists about the fate of *Rhizosolenia* in the open ocean, especially about the vertical distribution of losses due to grazing. Concentration of losses in the surface layer simulated possible grazing by copepods, euphausiids, and protozoans associated with dense surface aggregations of *Rhizosolenia* (Carpenter *et al.*, 1977; Villareal and Carpenter, 1989), as has been observed for the bloom-forming cyanobacterium *Trichodesmium* (O'Neil and Roman, 1992). This simulation assumes that the concentration of grazers will be directly correlated with

food supply (see Longhurst and Harrison, 1989). Concentration of losses in the bottom layer of the model simulated irreversible sinking of biomass from the euphotic zone, which might occur if cells were unable to recover from periods of nitrate depletion in surface waters, and any grazing that might occur due to concentration of zooplankton in deeper layers (see Venrick *et al.*, 1973). Considering the importance of the variation of loss rate with depth to the predicted fluxes of PC and PN due to migrations of *Rhizosolenia*, further research on associated loss processes is warranted.

*Relative contributions of Rhizosolenia migrations to nutrient cycling and new production in the open ocean*

Our model considered only one possible initial concentration of biomass when determining fluxes of PC and PN due to *Rhizosolenia* migrations. The relationship between fluxes of PC and PN and the initial abundance of *Rhizosolenia* can be described by:

$$\phi = F/C \quad (15)$$

where  $F$  is the net flux of PC or PN ( $\text{mmol m}^{-2} \text{ day}^{-1}$ ),  $C$  is the integrated water column abundance of *Rhizosolenia* in the form of PC or PN ( $\text{mmol m}^{-2}$ ) and  $\phi$  is the flux of PC or PN due to migrations of *Rhizosolenia* normalized to the initial biomass ( $\text{day}^{-1}$ ). Using values of net flux determined from the base model (see Table IV, VI or VII), the initial abundance of PC and PN, and equation (15), we calculate the value of  $\phi$  to be  $0.07 \text{ day}^{-1}$  for the net downward flux of PC and  $0.14 \text{ day}^{-1}$  for the net upward flux of PN. Values of  $\phi$  for variations of the base model are found in Table VIII. No matter what the initial abundance of biomass, multiplication of integrated water column abundance by  $\phi$  will yield an estimate of the net downward flux of PC or the net upward flux of PN, provided that the conditions in the water column are similar to those defined in the base model or to the chosen variation of the base model. The results of the model may also be used to help estimate integrated water column abundance. Using Table V, *Rhi-*

**Table VIII.** Calculated values of  $\phi$  (normalized flux,  $\text{day}^{-1}$ ) for variations of the *Rhizosolenia* migration model. The product of  $\phi$  and the integrated water column abundance ( $\text{mmol m}^{-2}$ ) of *Rhizosolenia* gives an estimate of the net downward flux of particulate carbon (PC) or net upward flux of particulate nitrogen (PN) due to *Rhizosolenia* migrations

Model variation	$\phi$ for PC	$\phi$ for PN
Base model	0.07	0.14
Top losses only	0.004	0.2
Bottom losses only	0.32	0
Top and bottom losses	0.16	0.11
Critical PC:PN 10.7, 7.1	0.08	0.14
Critical PC:PN 15.4, 8.3	0.08	0.14
$A, \Psi = 3 \text{ m h}^{-1}$	0.05	0.14
$A, \Psi = 6 \text{ m h}^{-1}$	0.10	0.19
$A, \Psi = 8 \text{ m h}^{-1}$	0.12	0.18

*zosolenia* found in the surface 10 m of the water column may represent between 15 and 39% of *Rhizosolenia*-derived PC, and between 15 and 36% of all *Rhizosolenia*-derived PN.

The potential relative contribution of migrations of *Rhizosolenia* to fluxes of PC and PN, and thus to oceanic new production, is estimated by calculating fluxes based on a range of abundances obtained in the open ocean. Data on the abundance and distribution of *Rhizosolenia*, horizontally, vertically and on basin-wide spatial scales, are limited. Kilometre-scale estimates of *Rhizosolenia* abundance in the North Pacific Gyre range from values of  $7.5 \times 10^{-4}$  mmol N m<sup>-3</sup> over the upper 4 m of the water column (Villareal and Carpenter, 1989) to  $1.75 \times 10^{-3}$  mmol N m<sup>-3</sup> over the top 16 m of the water column (Alldredge and Silver, 1982). These concentrations were converted from units of mats m<sup>-3</sup> using an average of  $2.5 \times 10^{-3}$  mmol N mat<sup>-1</sup> given by Villareal *et al.* (1996), although since the size of mats varies considerably (Villareal *et al.*, 1993), this value should be considered approximate.

In general, it is difficult to determine integrated water column abundance of *Rhizosolenia* as the vertical extent of *Rhizosolenia* mats must be measured by scuba divers who are limited to ~20 m of vertical descent. If we assume that the concentration of *Rhizosolenia* observed by Alldredge and Silver (1982) ( $1.75 \times 10^{-3}$  mmol N m<sup>-3</sup>) occurs over the top 20 m of the water column instead of the top 16 m, and if we assume that this biomass represents ~21% of the integrated water column abundance (see Table V), the integrated water column abundance will be ~0.17 mmol N m<sup>-2</sup>. Using equation (15) and the range of values of  $\phi$  shown in Table VIII (0.11–0.2; this does not include the zero value for the model where losses were concentrated in the bottom layer which would result in a calculated flux of zero), the estimated net upward flux of nitrogen to the euphotic zone would range between 0.018 and 0.033 mmol N m<sup>-2</sup> day<sup>-1</sup>. From here on, we will use a net upward flux of 0.033 mmol N m<sup>-2</sup> day<sup>-1</sup> as the maximum potential contribution of migrations of *Rhizosolenia* to new production in the open ocean. This value is within the range of previous estimates. Villareal *et al.* (1996) calculated the gross upward flux of nitrate due to *Rhizosolenia* migrations to be between 0.004 and 0.040 mmol N m<sup>-2</sup> day<sup>-1</sup>; however, this calculation did not consider the nitrogen that would return to deep water during the downward phase of the migration cycle. Because it was calculated using a slightly lower abundance of PN, the values are similar to ours.

The importance of the predicted upward flux of N to total new production in open-ocean regions can be estimated by comparing the predicted net upward flux of PN from the model to estimates of new production that results from turbulent diffusion of nitrate into the euphotic zone, to new production from nitrogen fixation, and to estimates of export production from sediment traps. Estimates of the flux of nitrate into the euphotic zone of the oligotrophic ocean due to the turbulent diffusion vary by more than two orders of magnitude, ranging from 0.003 mmol N m<sup>-2</sup> day<sup>-1</sup> (Carr *et al.*, 1995) to 1.644 mmol N m<sup>-2</sup> day<sup>-1</sup> (Jenkins, 1988) (see Table IX). Not including the lowest (Carr *et al.*, 1995) and highest (Jenkins, 1988) fluxes, an average of these values is ~0.2 mmol N m<sup>-2</sup> day<sup>-1</sup>. Thus, new production that results from migrations of *Rhizosolenia* (0.033 mmol N m<sup>-2</sup> day<sup>-1</sup>)

Potential contributions of *Rhizosolenia* to nutrient cycling

**Table IX.** Estimates of new production from turbulent fluxes of nitrate into the euphotic zone and nitrogen fixation, and nitrogen-based estimates of export production for comparison with vertical fluxes of N due to migrations of *Rhizosolenia* in the open ocean

Source of new production	Location	New production (mmol m <sup>-2</sup> day <sup>-1</sup> )	Reference
Turbulent nitrate flux	Sargasso Sea	0.022–0.134	McCarthy and Carpenter, 1983
	Western Pacific	0.25–0.31	Peña <i>et al.</i> , 1994
	Warm Pool		
	Eastern Atlantic	0.27	Ledwell <i>et al.</i> , 1993
	26°N, 28°W		
	Sargasso Sea	1.644	Jenkins, 1988
	Eastern Atlantic	0.139	Lewis <i>et al.</i> , 1986
Nitrogen fixation	28.5°N, 23°W		
	Equatorial Pacific	0.003	Carr <i>et al.</i> , 1995
	10°N, 150°W		
Export production	Northeast Pacific	0.594	Harrison <i>et al.</i> , 1992
	33°N, 139°W		
	North Atlantic	0.038	Goering <i>et al.</i> , 1966
	Caribbean	0.077	Carpenter and Price, 1977
	Sargasso Sea	0.0014	Carpenter and McCarthy, 1975
<i>Rhizosolenia</i> migrations	North Pacific	0.46	Martin <i>et al.</i> , 1987
	Subtropical Gyre		
	Sargasso Sea	0.77	Michaels <i>et al.</i> , 1994
	North Pacific	0.714	Karl and Knauer, 1984
	Subtropical Gyre		
	North Pacific Gyre	0.427	Harrison <i>et al.</i> , 1992
	Modelled	0.018–0.033	This study

may be up to 17% of new production that results from diffusive fluxes of nitrogen into the euphotic zone. It is important to note that comparisons should be made with caution as the variation in turbulent fluxes of nitrate is extremely high. Estimates of new production from nitrogen fixation are less variable than those from turbulent fluxes of nitrate, but variation still exists (Table IX). If 0.025 mmol N m<sup>-2</sup> day<sup>-1</sup> is used as an estimate, then the net upward flux of N to the euphotic zone due to migrations may be 1.3 times higher than the new production due to nitrogen fixation.

The variability in estimates of new (export) production from sediment trap measurements in both the Atlantic and Pacific Oceans is somewhat less than the variability in turbulent fluxes of nitrate (see Table IX), although fewer measurements exist. At best, new production due to migrations of *Rhizosolenia* represents ~8% of new production as measured by sediment traps, using estimates of 0.46 mmol N m<sup>-2</sup> day<sup>-1</sup> (Martin *et al.*, 1987) and 0.43 mmol N m<sup>-2</sup> day<sup>-1</sup> (Harrison *et al.*, 1992). Export production expressed as fluxes of carbon can also be compared to the net downward flux of PC predicted by the model. Values predicted by the model range from 0.0008 to 0.058 mmol C m<sup>-2</sup> day<sup>-1</sup>. If we compare these values to carbon-based estimates of export production from sediment traps in the Pacific Ocean by Martin *et al.* (1987) (~4.1 mmol C m<sup>-2</sup> day<sup>-1</sup>), export production due to migrations of *Rhizosolenia* is <2% of sediment trap estimates.

Contributions of migrations of *Rhizosolenia* to open-ocean new production are limited by their relatively low standing crop. At a VERTEX station in the Central North Pacific Gyre, Karl and Knauer (1984) found the standing crop of PN to be 16 mmol m<sup>-2</sup> over the top 100 m of the water column, while Harrison *et al.* (1992) measured the standing crop of PN to be 36.3 mmol m<sup>-2</sup> over the top 150 m. These values are roughly two orders of magnitude higher than the highest estimates of integrated water column abundance of *Rhizosolenia* (0.17 mmol m<sup>-2</sup>) which consider that, according to the model, *Rhizosolenia* found in surface waters may account for only 21% of the total water column biomass. Additional measurements of *Rhizosolenia* abundance would greatly improve our efforts to predict their contributions to nutrient cycling.

Although we predict the potential contributions of *Rhizosolenia* migrations to overall levels of new production to be relatively small, they are potentially ecologically important. New production due to *Rhizosolenia* migrations can result in a disproportionately high net removal of carbon from oceanic surface waters, because *Rhizosolenia* migrations occur in regions where sources of light and nutrients are spatially separated. Often, nitrate does not become detectable until well below the euphotic zone (see Hayward, 1991); thus, uptake of nitrate by migrating *Rhizosolenia* will occur in the dark and, since photosynthesis requires light, the uptake of nitrate will not be accompanied by the uptake of carbon (see Richardson *et al.*, 1996). Thus, nitrate transported to the surface by migrating diatoms will not be accompanied by the stoichiometric equivalents of carbon. Nitrate entering the euphotic zone through physical transport of dissolved nutrients brings carbon with it in approximately the Redfield ratio (Redfield, 1958; Eppley and Peterson, 1979). Since photosynthesis at the surface requires a carbon source, and since carbon is not brought to the surface in coupled transport with nitrogen during vertical migrations, photosynthesis in upper layers may result in a net decrease in carbon from these layers (see also Fraga *et al.*, 1992). The uncoupled uptake of carbon and nitrogen during vertical migrations of *Rhizosolenia* is potentially the greatest contribution that these migrations can make to biogeochemical cycling and new production. Our model shows the uncoupling of C and N clearly, both by the predicted vertical distributions of PC and PN, and by the predicted fluxes, although the difference in the percentage of total biomass of PC compared to PN was only 1–2%.

In summary, this paper describes a numerical model constructed to estimate the potential contributions of *Rhizosolenia* migrations to nutrient cycling in the open ocean. New production that results from vertical migrations of *Rhizosolenia* may be up to 17% of that resulting from upward fluxes of nitrate due to turbulent diffusion, is approximately the same order of magnitude as contributions due to nitrogen fixation, and up to 8% of export production as measured by sediment traps. The contributions of *Rhizosolenia* migrations to nutrient cycling in the open ocean are relatively low. However, the uncoupled transport of carbon and nitrogen during migrations makes them of ecological and biogeochemical interest, as growth of *Rhizosolenia* at the surface fuelled by nitrate acquired below the euphotic zone may result in the net removal of carbon from oceanic surface waters.

### Acknowledgements

We thank A.J.Bowen, J.S.Craigie, W.G.Harrison and three helpful reviewers for comments on the manuscript. Many thanks to R.F.Davis for computer time and to R.M.Moore for interim funding. This study was supported in part by grants from the Natural Sciences and Engineering Research Council of Canada and the Office of Naval Research (J.J.C.), and a Dalhousie Graduate Scholarship (T.L.R.). This is the Center for Environmental Observation Technology and Research (CEOTR) publication number 14.

### References

- Allredge, A.L. and Silver, M.W. (1982) Abundance and production rates of floating diatom mats (*Rhizosolenia castracanei* and *R. imbricata* var. *shrubsolei*) in the Eastern Pacific Ocean. *Mar. Biol.*, **66**, 83–88.
- Beers, J.R., Reid, F.M.H. and Stewart, G.L. (1975) Microplankton of the North Pacific Central Gyre. Population structure and abundance, June 1973. *Int. Rev. Ges. Hydrobiol.*, **60**, 607–638.
- Bowman, T.E. and Lancaster, L.J. (1965) A bloom of the planktonic blue-green alga, *Trichodesmium erythraeum*, in the Tonga Islands. *Limnol. Oceanogr.*, **10**, 291–292.
- Carpenter, E.J. and McCarthy, J.J. (1975) Nitrogen fixation and uptake of combined nitrogenous nutrients by *Oscillatoria* (*Trichodesmium*) *thiebautii* in the western Sargasso Sea. *Limnol. Oceanogr.*, **20**, 389–401.
- Carpenter, E.J. and Price, C. (1977) Nitrogen fixation, distribution, and production of *Oscillatoria* (*Trichodesmium*) spp. in the western Sargasso and Caribbean Seas. *Limnol. Oceanogr.*, **22**, 60–72.
- Carpenter, E.J. and Romans, K. (1991) Major role of the cyanobacterium *Trichodesmium* in nutrient cycling in the North Atlantic Ocean. *Science*, **254**, 1356–1358.
- Carpenter, E.J., Harbison, G.R., Madin, L.P., Swanberg, N.R., Biggs, D.C., Hulburt, E.M., McAlister, V.L. and McCarthy, J.J. (1977) *Rhizosolenia* mats. *Limnol. Oceanogr.*, **22**, 739–741.
- Carr, M.-E., Lewis, M.R., Kelley, D. and Jones, B. (1995) A physical estimate of new production in the Equatorial Pacific along 150°W. *Limnol. Oceanogr.*, **40**, 138–147.
- Chisholm, S.W. (1992) Phytoplankton size. In Falkowski, P.G. and Woodhead, A.D. (eds), *Primary Productivity and Biogeochemical Cycles in the Sea*. Plenum Press, New York, pp. 299–316.
- Cullen, J.J., Geider, R.J., Ishizaka, J., Kiefer, D.A., Marra, J., Sakshaug, E. and Raven, J.A. (1993) Toward a general description of phytoplankton growth for biogeochemical models. In Evans, G.T. and Fasham, M.J.R. (eds), *Towards a Model of Ocean Biogeochemical Processes*. NATO ASI Series, Vol. 10. Springer-Verlag, Berlin, pp. 153–176.
- Dugdale, R.C. and Goering, J.J. (1967) Uptake of new and regenerated forms of nitrogen in primary productivity. *Limnol. Oceanogr.*, **12**, 196–206.
- Eppley, R.W. and Peterson, B.J. (1979) Particulate organic matter flux and planktonic new production in the deep ocean. *Nature*, **282**, 677–680.
- Fasham, M.J.R., Ducklow, H.W. and McKelvie, S.M. (1990) A nitrogen-based model of plankton dynamics in the oceanic mixed layer. *J. Mar. Res.*, **48**, 591–639.
- Fraga, F., Pérez, F.F., Figueiras, F.G. and Rios, A.F. (1992) Stoichiometric variations of N, P, C, and O<sub>2</sub> during a *Gymnodinium catenatum* red tide and their interpretation. *Mar. Ecol. Prog. Ser.*, **87**, 123–134.
- Geider, R.J. (1992) Respiration: taxation without representation? In Falkowski, P.G. and Woodhead, A.D. (eds), *Primary Productivity and Biogeochemical Cycles in the Sea*. Plenum Press, New York, pp. 333–360.
- Goering, J.J., Dugdale, R.C. and Wenzel, D.W. (1966) Estimates of *in situ* rates of nitrogen uptake by *Trichodesmium* sp. in the tropical Atlantic Ocean. *Limnol. Oceanogr.*, **11**, 614–621.
- Goldman, J.C. (1988) Spatial and temporal discontinuities of biological processes in pelagic surface waters. In Rothschild, B.J. (ed.), *Toward a Theory on Biological-Physical Interactions in the World Ocean*. Kluwer Academic, Dordrecht, pp. 273–296.
- Harrison, W.G., Harris, L.R., Karl, D.M., Knauer, G.A. and Redalje, D.G. (1992) Nitrogen dynamics at the VERTEX time-series site. *Deep-Sea Res.*, **39**, 1525–1552.
- Hayward, T.L. (1991) Primary production in the North Pacific Central Gyre: a controversy with important implications. *Trends Ecol. Evol.*, **6**, 281–284.

- Hayward, T.L. (1994) The shallow oxygen maximum layer and primary production. *Deep-Sea Res.*, **41**, 559–574.
- Jenkins, W.J. (1988) Nitrate flux into the euphotic zone near Bermuda. *Nature*, **331**, 521–523.
- Karl, D.M. and Knauer, G.A. (1984) Vertical distribution, transport, and exchange of carbon in the northeast Pacific Ocean: evidence for multiple zones of biological activity. *Deep-Sea Res.*, **31**, 221–243.
- Karl, D.M., Letelier, R., Hebel, D.V., Bird, D.F. and Winn, C.D. (1992) *Trichodesmium* blooms and new nitrogen in the North Pacific Gyre. In Carpenter, E.J., Capone, D.G. and Reuter, J.G. (eds), *Marine Pelagic Cyanobacteria: Trichodesmium and Other Diazotrophs*. Kluwer Academic, Boston, pp. 219–237.
- Kirk, J.T.O. (1994) *Light and Photosynthesis in Aquatic Ecosystems*, 2nd edn. Cambridge University Press, Cambridge, 509 pp.
- Kromkamp, J. and Walsby, A.E. (1990) A computer model of buoyancy and vertical migration in cyanobacteria. *J. Plankton Res.*, **12**, 161–183.
- Ledwell, J.R., Watson, A.J. and Law, C.S. (1993) Evidence for slow mixing across the pycnocline from an open-ocean tracer-release experiment. *Nature*, **364**, 701–703.
- Lewis, M.R., Harrison, W.G., Oakey, N.S., Hebert, D. and Platt, T. (1986) Vertical nitrate fluxes in the oligotrophic ocean. *Science*, **234**, 870–873.
- Li, W.K.W. and Morris, I. (1982) Temperature adaptation in *Phaeodactylum tricoratum* Bohlin: Photosynthetic rate compensation and capacity. *J. Exp. Mar. Biol. Ecol.*, **58**, 135–150.
- Longhurst, A.R. and Harrison, W.G. (1989) The biological pump: Profiles of plankton production and consumption in the upper ocean. *Prog. Oceanogr.*, **22**, 47–123.
- Martin, J.H., Knauer, G.A., Karl, D.M. and Broenkow, W.W. (1987) VERTEX: Carbon cycling in the northeast Pacific. *Deep-Sea Res.*, **34**, 267–285.
- Martinez, L., Silver, M.W., King, J.M. and Alldredge, A.L. (1983) Nitrogen fixation by floating diatom mats: a source of new nitrogen to oligotrophic ocean waters. *Science*, **221**, 152–154.
- McCarthy, J.J. and Carpenter, E.J. (1983) Nitrogen cycling in near-surface waters of the open ocean. In Carpenter, E.J. and Capone, D.G. (eds), *Nitrogen in the Marine Environment*. Academic Press, New York, pp. 487–512.
- Michaels, A.F., Bates, N.R., Buesseler, K.O., Carlson, C.A. and Knap, A.H. (1994) Carbon cycle imbalances in the Sargasso Sea. *Nature*, **372**, 537–540.
- Moore, J.K. and Villareal, T.A. (1996a) Buoyancy and growth characteristics of three positively buoyant marine diatoms. *Mar. Ecol. Prog. Ser.*, **132**, 203–213.
- Moore, J.K. and Villareal, T.A. (1996b) Size-ascent rate relationships in positively buoyant marine diatoms. *Limnol. Oceanogr.*, **41**, 1514–1520.
- Morel, A. (1978) Available, usable, and stored radiant energy in relation to marine photosynthesis. *Deep-Sea Res.*, **25**, 673–688.
- Munk, W.H. and Riley, G.A. (1952) Absorption of nutrients by aquatic plants. *J. Mar. Res.*, **11**, 215–240.
- O’Neil, J.M. and Roman, M.R. (1992) Grazers and associated organisms of *Trichodesmium*. In Carpenter, E.J., Capone, D.G. and Reuter, J.G. (eds), *Marine Pelagic Cyanobacteria: Trichodesmium and Other Diazotrophs*. Kluwer Academic, Boston, pp. 61–73.
- Pasciak, W.J. and Gavis, J. (1974) Transport limitation of nutrient uptake in phytoplankton. *Limnol. Oceanogr.*, **19**, 604–617.
- Peña, M.A., Lewis, M.R. and Cullen, J.J. (1994) New production in the warm waters of the tropical Pacific Ocean. *J. Geophys. Res.*, **99**, 14255–14268.
- Platt, T., Gallegos, C.L. and Harrison, W.G. (1980) Photoinhibition of photosynthesis in natural assemblages of marine phytoplankton. *J. Mar. Res.*, **38**, 687–701.
- Redfield, A.C. (1958) The biological control of chemical factors in the environment. *Am. Sci.*, **46**, 1–18.
- Richardson, T.L. and Cullen, J.J. (1995) Changes in buoyancy and chemical composition during growth of a coastal marine diatom: ecological and biogeochemical consequences. *Mar. Ecol. Prog. Ser.*, **128**, 77–90.
- Richardson, T.L., Ciotti, A.M., Cullen, J.J. and Villareal, T.A. (1996) Physiological and optical properties of *Rhizosolenia formosa* (Bacillariophyceae) in the context of open-ocean vertical migration. *J. Phycol.*, **32**, 741–757.
- Smayda, T.J. (1970) The suspension and sinking of phytoplankton in the sea. *Oceanogr. Mar. Biol. Annu. Rev.*, **8**, 353–414.
- Venrick, E.L., McGowan, J.A. and Mantyla, A.W. (1973) Deep maxima of photosynthetic chlorophyll in the Pacific Ocean. *Fish. Bull.*, **71**, 41–52.
- Villareal, T.A. (1987) Evaluation of nitrogen fixation in the diatom genus *Rhizosolenia* Eh. in the absence of its cyanobacterial symbiont *Richelia intracellularis* Schmidt. *J. Plankton Res.*, **9**, 965–971.

#### Potential contributions of *Rhizosolenia* to nutrient cycling

- Villareal, T.A. (1988) Positive buoyancy in the oceanic diatom *Rhizosolenia debyana* H. Peragallo. *Deep-Sea Res.*, **35**, 1037–1045.
- Villareal, T.A. (1992) Buoyancy properties of the giant diatom *Ethmodiscus*. *J. Plankton Res.*, **14**, 459–463.
- Villareal, T.A. and Carpenter, E.J. (1989) Nitrogen fixation, suspension characteristics, and chemical composition of *Rhizosolenia* mats in the Central North Pacific Gyre. *Biol. Oceanogr.*, **6**, 327–345.
- Villareal, T.A. and Carpenter, E.J. (1990) Diel buoyancy regulation in the marine diazotrophic cyanobacterium *Trichodesmium thiebautii*. *Limnol. Oceanogr.*, **35**, 1832–1837.
- Villareal, T.A. and Carpenter, E.J. (1994) Chemical composition and photosynthetic characteristics of *Ethmodiscus rex* (Bacillariophyceae): Evidence for vertical migration. *J. Phycol.*, **30**, 1–8.
- Villareal, T.A. and Lipschultz, F. (1995) Internal nitrate concentrations in single cells of large phytoplankton from the Sargasso Sea. *J. Phycol.*, **31**, 689–696.
- Villareal, T.A., Altabet, M.A. and Culver-Rymsza, K. (1993) Nitrogen transport by vertically migrating diatom mats in the North Pacific Ocean. *Nature*, **363**, 709–712.
- Villareal, T.A., Woods, S., Moore, J.K. and Culver-Rymsza, K. (1996) Vertical migration of *Rhizosolenia* mats and their significance to  $\text{NO}_3^-$  fluxes in the central North Pacific gyre. *J. Plankton Res.*, **18**, 1103–1121.
- Yoder, J.A., Ackleson, S.G., Barber, R.T., Flament, P. and Balch, W.M. (1994) A line in the sea. *Nature*, **371**, 689–692.

Received on September 30, 1996; accepted on September 26, 1997